Supporting Information

Upconverting mixed emitter nanocomposites as sensitive luminescent thermometers within plant-inspired artificial fliers

Albenc Nexha,[1] **Stefano Mariani**,[2] **Anja Colbus**,[1] **Kliton Cikalleshi**,[2,3] **Barbara Mazzolai**[2*] **and Tobias Kraus**[1,4*]

[1]*INM-Leibniz Institute for New Materials, 66123 Saarbrücken, Germany*
[2]*Bioinspired Soft Robotics Laboratory, Istituto Italiano di Tecnologia, Italy*
[3]*The Biorobotics Institute, Scuola Superiore Sant'Anna, 56025 Pontedera, Italy*
[4]*Saarland University, Colloid and Interface Chemistry, 66123 Saarbrücken, Germany*
*tobias.kraus@leibniz-inm.de
*barbara.mazzolai@iit.it

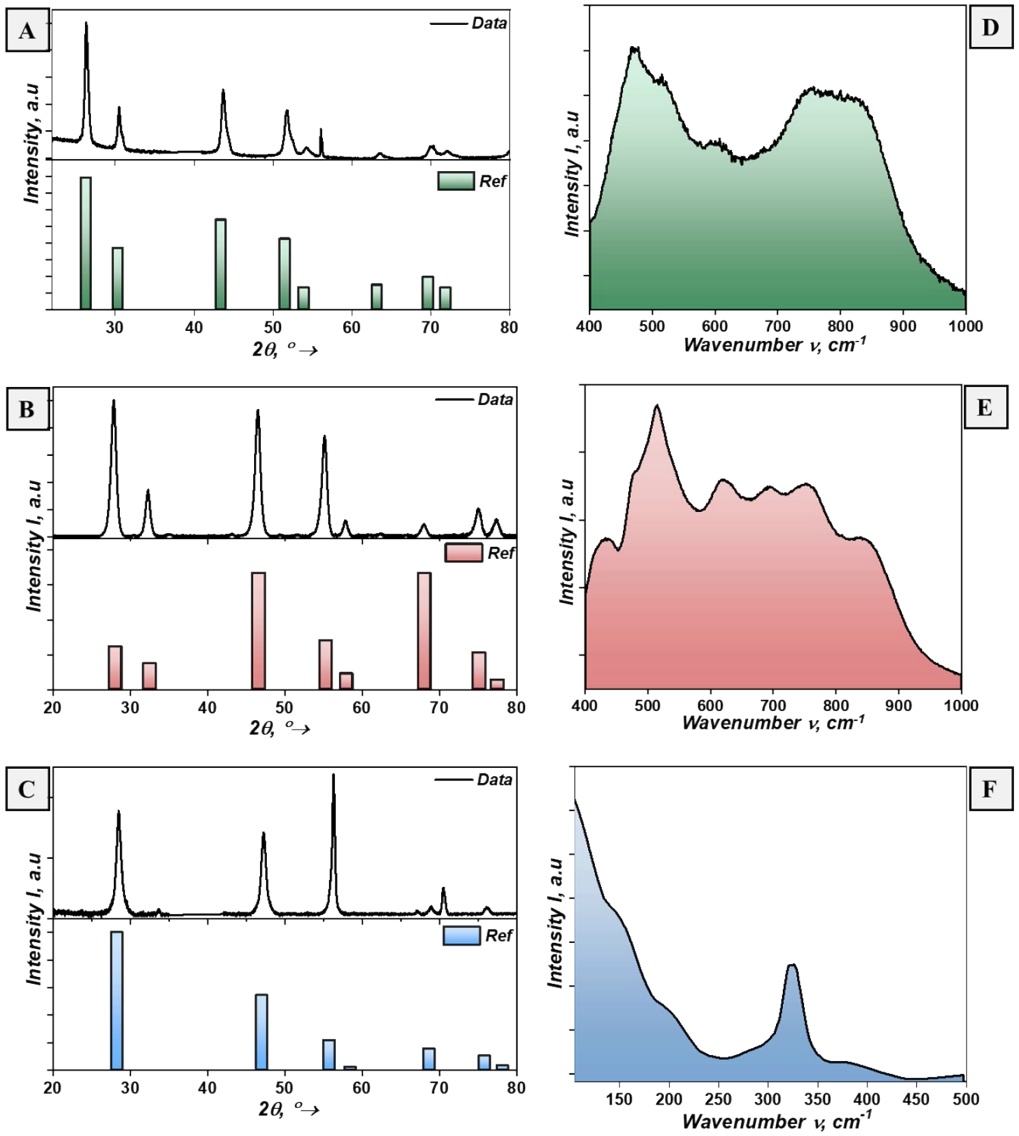

Fig. S1. X-ray diffraction patterns and Raman vibration modes of: (A), (D) $BaYF_5$ for green emitters, (B), (E) $NaYF_4$ for red emitters, and (C), (F) CaF_2 for blue emitters.

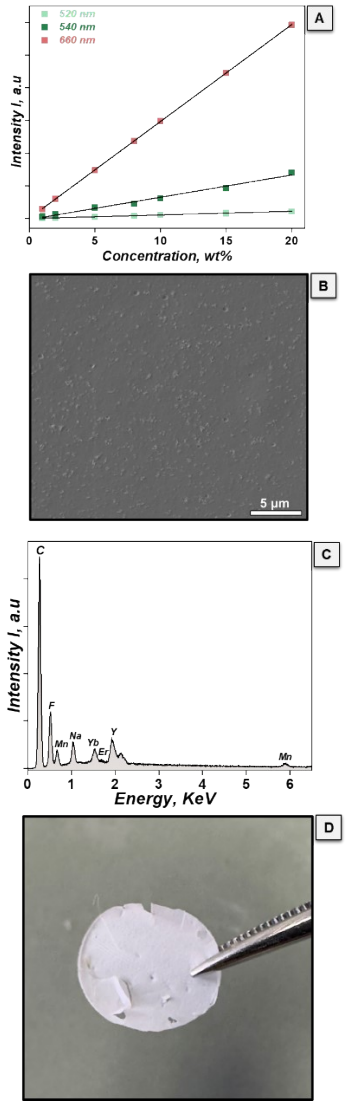

Fig. S2. Optimizing the concentration of the upconverting particles in composites. (A) Concentration-dependant emissions of red emitting Mn^{2+}, Er^{3+}, Yb^{3+} in $NaYF_4$ in PHA polymer as an example, (B) SEM image and (C) EDX spectra of 15 wt% red emitting particles in PHA. (D) Digital image of a fluorescent composite prepared with 20 wt% red emitting particles to illustrate the effect of excessive filler loading on the mechanical properties of the composite.

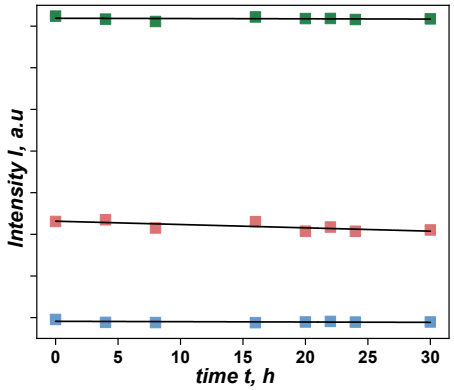

Fig. S3. Photostability of the blue, green and red fluorescent nanocomposites as a function of time (0 to 30 hours) while continuously irradiating with 980 nm operating at 0.4 W/cm^2.

Section S1. Thermometric performance of single fluorescent composites

The thermometric performance of the single emitting fluorescent nanocomposites (green, red and blue) is governed by thermally coupled levels (TCLs) because the energy gaps (ΔE) between their emitting levels are within the range from 200 cm^{-1} to 2000 cm^{-1}. The variation of the intensities of the TCLs per each fluorescent nanocomposites with the temperature was monitored within the environmental temperature range (268 K to 313 K, green emitters as a model, Fig. S4 (A)). For the green nanocomposites, TCLs are located at 520 nm (as I_1) and 540 nm (as I_2) (Fig. S4 (B)). For the red nanocomposites, TCLs are located at 650 nm (as I_1) and 660 nm (as I_2) (Fig. S4 (C)). For the blue composites, TCLs are located at 450 nm (as I_1) and 475 nm (as I_2) (Fig. S4 (D)).

The intensity ratio (Δ) of these TCLs obeys the Boltzmann law as follows:

$$\Delta = B\, exp\left(-\frac{\Delta E}{k_B T}\right) \qquad (S1)$$

where ΔE is the energy gap between the two energy levels responsible for emissions, k_B is Boltzmann's constant, T is the temperature in Kelvin, and B a constant to be determined from the experimental fitting. Substituting Equation S1 in the expression for the calculation of the relative thermal sensitivity (S_{rel}):

$$S_{rel} = \frac{1}{\Delta}\left|\frac{\partial \Delta}{\partial T}\right| \cdot 100\% \qquad (S2)$$

The final equation for the calculation of S_{rel} for TCLs is as follows:

$$S_{rel} = \left|\frac{\Delta E}{k_B T^2}\right| \cdot 100\% \qquad (S3)$$

This equation implies that S_{rel} is directly proportional to the experimental ΔE and can be improved only at cryogenic temperatures.

Per each of the fluorescent composites, the integrated area of the emission bands involved into the thermal sensing, are extracted as a function of temperature. The variation of Δ as a function of temperature displays a continuous increase with temperature (Fig. S4 (E)). The experimentally measured Δ were fitted to Equation S1 to obtain ΔE, and S_{rel} were calculated using Equation S3, $S_{rel}$for the green, red, and blue single fluorescent nanocomposites.

Green: $\Delta = 0.91\, exp\left(-\frac{705}{k_B T}\right)$; Red: $\Delta = 1.62\, exp\left(-\frac{255}{k_B T}\right)$; Blue: $\Delta = 5.80\, exp\left(-\frac{1302}{k_B T}\right)$

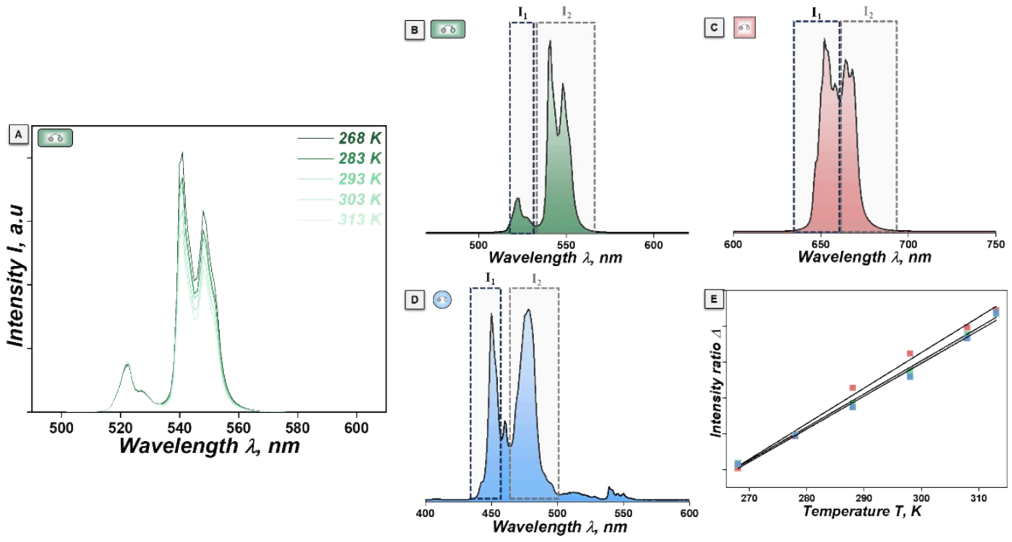

Fig. S4. Luminescent thermometry with single emitting fluorescent nanocomposites: (A) photoluminescence as a function of temperature (268 K to 313 K for the green emitters as a model). Selected emission wavelengths for thermal sensing in (B):

green, (C) red, and (D) blue nanocomposites. (E) Temperature dependence of the intensity ratio Δ for the green (in green symbols), red (in red symbols) and blue (in blue symbols) nanocomposites. The green (Er^{3+}, Yb^{3+}:$BaYF_5$), red (Mn^{2+}, Er^{3+}, Yb^{3+}:$NaYF_4$), and blue (Er^{3+}, Tm^{3+}:CaF_2) nanoparticles are depicted in green rectangle, red square and blue sphere, respectively.

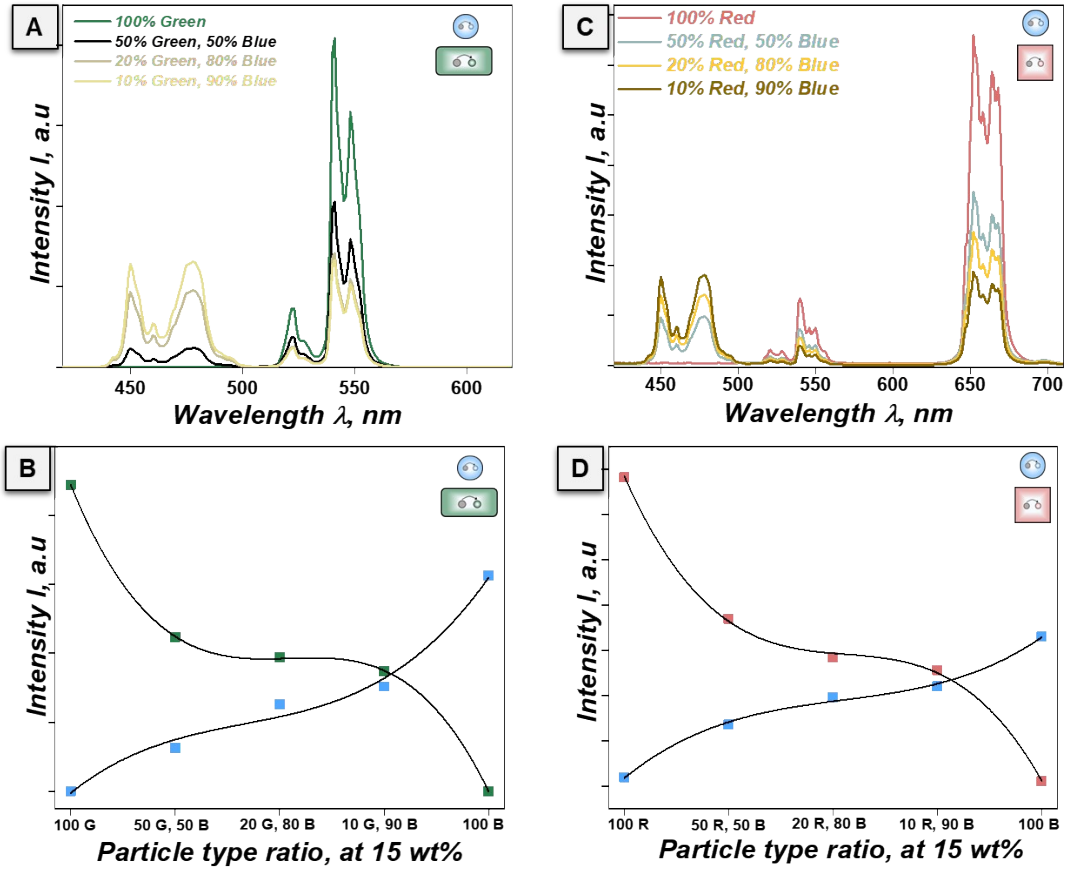

Fig. S5. Upconversion spectra and intensities of PHA composites with different ratios of upconverting particles upon excitation with a 980 nm laser operating at 0.4 W/cm². Emissions at 475 nm (blue), 540 nm (green), and 650 nm (red) are shown for composites containing (A), (B) blue Tm^{3+}, Yb^{3+}:CaF_2 ("B" for "*Blue*") and green Er^{3+}, Yb^{3+}:$BaYF_5$ ("G" for "*Green*") nanoparticles, and (C), (D) blue Tm^{3+}, Yb^{3+}:CaF_2 and red Mn^{2+} doped Er^{3+}, Yb^{3+}:$NaYF_4$ ("R" for "*Red*") nanoparticles. All composites had an overall filling ratio of 15 wt%.

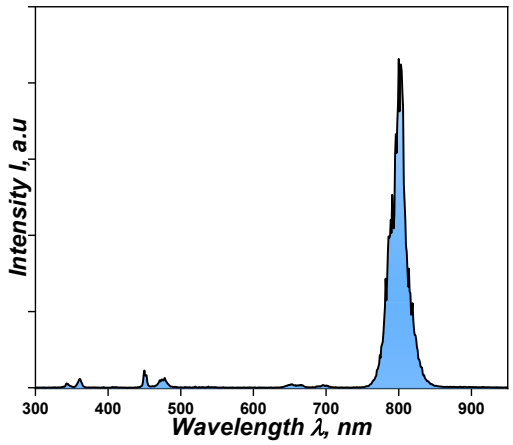

Fig. S6. Full range upconverting spectra of Tm^{3+}, Yb^{3+}:CaF_2 nanoparticles under 980 nm excitation with a power density of 0.4 W/cm^2.

Section S2. Thermometric performance of mixed fluorescent composites

The photoluminescence of the mixed composites was monitored within the temperature range from 268 K to 313 K. The area of each of the emission bands within the selected compositions was integrated as a function of temperature (Fig. S7). The thermometric parameter Δ was set as the ratio between the intensity of the blue vs. the green wavelength (Δ_1), blue vs. the red wavelength (Δ_2), and green vs. the red wavelength (Δ_3). The experimental data were best fitted by the following equation:

$$\Delta_i = \frac{a_i + b_i T}{1 + c_i T + d_i T^2} \qquad (S4)$$

where a_i, b_i, c_i, and d_i are constants to be determined from the fitting.

The thermometric performance of these mixed composites can be evaluated by calculating the thermal sensitivities (the absolute S_{abs} and the relative S_{rel}), the δT and the repeatability R. S_{abs} is the first derivative of the thermometric parameter:

$$S_{abs} = \frac{\partial \Delta}{\partial T} = \left(\frac{b_i}{1 + c_i T + d_i T^2} - \frac{(a_i + b_i T) * (c_i + 2 d_i T)}{\left(1 + c_i T + d_i T^2\right)^2} \right) \qquad (S5)$$

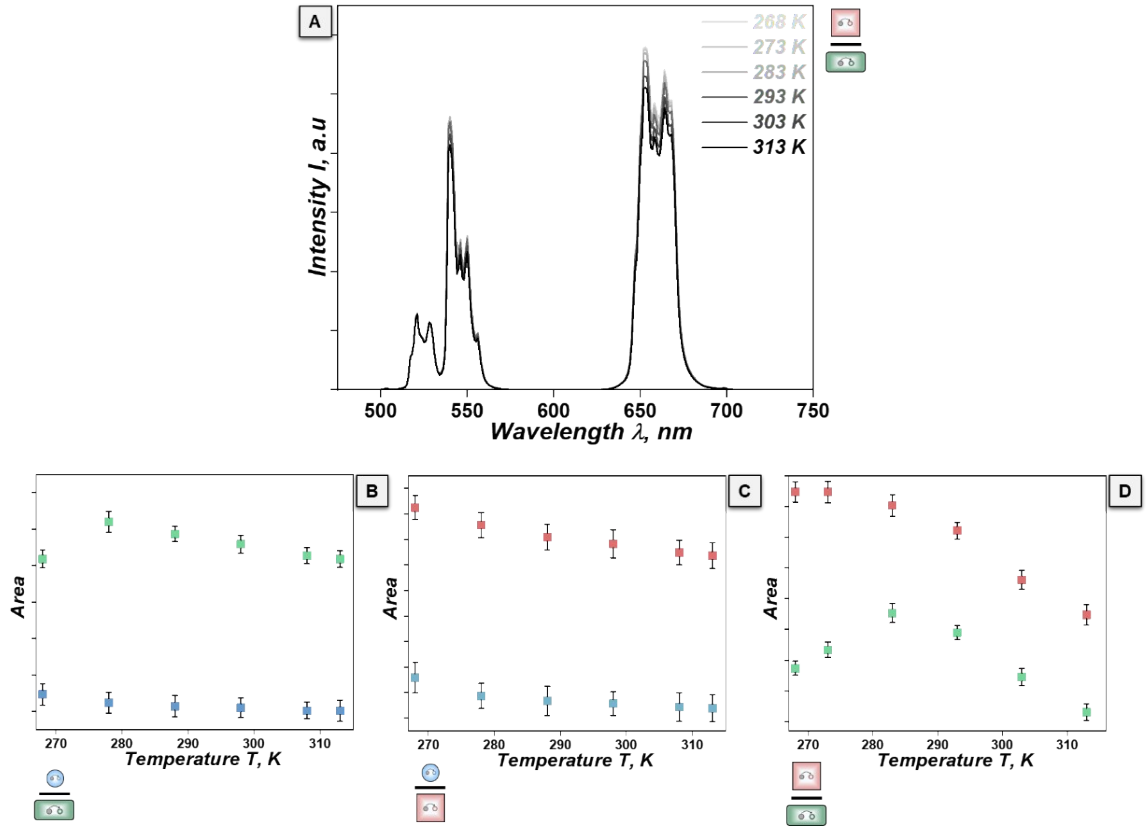

Fig. S7. Luminescent thermometry with mixed emitting fluorescent nanocomposites: (A) photoluminescence emission as a function of temperature (268 K to 313 K for the green and red emitters are shown as a model). Integrated areas of the mixed emitting fluorescent nanocomposites: (B) blue and green ($^{\Delta_1}$), (C) blue and red ($^{\Delta_2}$), and (D) green and blue ($^{\Delta_3}$), as a function of temperature.

The expression for $^{S_{rel}}$ after substituting Equation S6 to Equation S5 becomes:

$$S_{rel(i)} = \frac{1 + c_i T + d_i T^2}{(a_i + b_i T)} * \left(\frac{b_i}{1 + c_i T + d_i T^2} - \frac{(a_i + b_i T) * (c_i + 2 d_i T)}{\left(1 + c_i T + d_i T^2\right)^2} \right) \cdot 100\% \quad (S6)$$

We can also estimate the $^{\delta T}$ of these composites via:[1, 2]

$$\delta T_i = \frac{1}{S_{rel(i)}} \frac{\delta \Delta}{\Delta_i} \quad (S7)$$

where $\frac{\delta \Delta}{\Delta}$ is the uncertainty on determining the thermometric parameter, estimated by the manufacturer as 0.5% for the type of detector that we have used to record the data.[1, 2] Finally, the repeatability) was determined using:[1, 2]

$$R_i = 1 - \frac{max|\Delta_c - \Delta_i|}{\Delta_c} \quad (S8)$$

where $^{\Delta_c}$ is the mean thermometric parameter and $^{\Delta_i}$ are the values of the individual measurements of the thermometric parameter using different heating/cooling cycles shown below. All results are summarised in Fig. S**8** and Table S1.

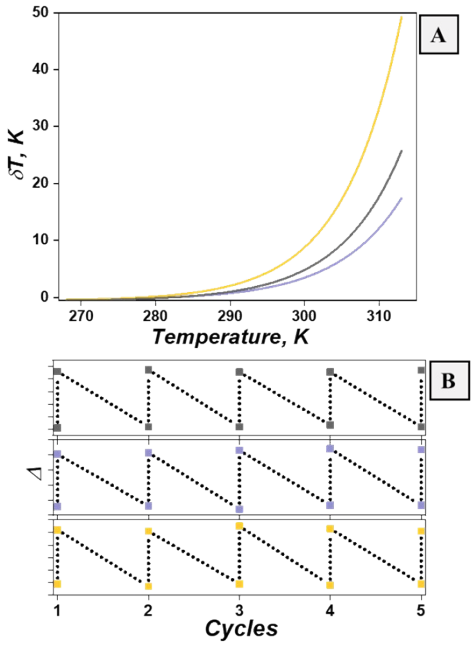

Fig. S8. (A) Temperature resolution and (B) the repeatability of the data for the mixed nanocomposites. Purple, yellow and grey symbols and lines stand for the mixture of blue/green ($^{\Delta}1$), blue/red ($^{\Delta}2$), and green/red ($^{\Delta}3$), respectively.

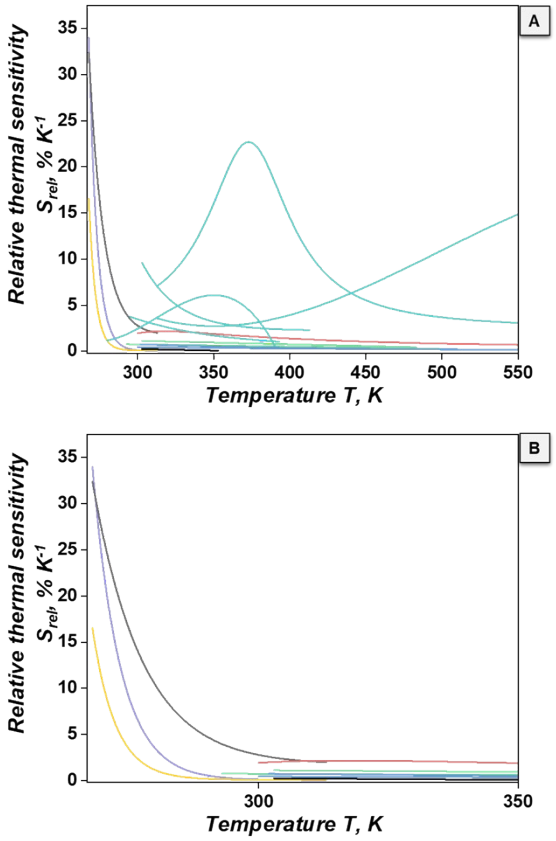

Fig. S9. S_{rel} of mixed composites (in grey, magenta and yellow lines) compared with state of the art thermometers: (A) TCLs and NTCLs thermometers, and (B) only TCLs thermometers. TCLs of green (green lines), red (red lines), blue (blue lines), and NIR emitters (black line) and NTCLs (in turquoise lines).

A

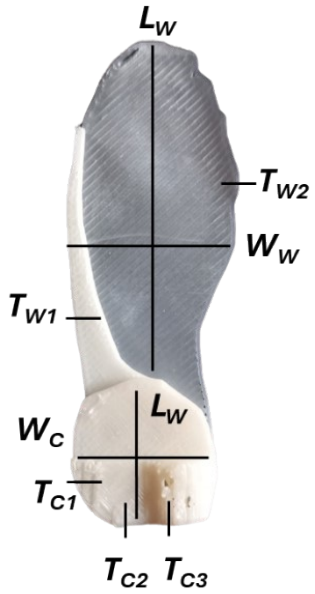

B

Parameter	Artificial seed
N sample	3
L_w (mm)	40.6 ± 0.15
W_w (mm)	20.8 ± 0.02
T_{w1} (mm)	0.66 ± 0.02
T_{w2} (mm)	0.11 ± 0.01
L_c (mm)	17.0 ± 0.30
W_c (mm)	16.7 ± 0.30
T_{c1} (mm)	2.59 ± 0.03
T_{c2} (mm)	3.76 ± 0.04
T_{c3} (mm)	5.35 ± 0.08

Fig. S10. (A) Picture and (B) table with the morphological characteristics of the artificial *Acer campestre* seed.

Table S1. Summary of the thermometric performance of the mixed fluorescent nanocomposites. The values of S_{rel} and δT are reported at 268 K.

Composite	Δ	a	b	c	d	R^2	S_{rel} **(% K^{-1})**	δT **(K)**	R **(%)**
Blue-Green	Δ_1	8.086	-0.0303	-0.00200	-6.64E^{-6}	0.99	33.9	0.014	97
Blue-Red	Δ_2	0.4195	-0.00157	-0.00221	-5.75E^{-6}	0.99	16.5	0.030	98
Green-Red	Δ_3	1.5507	-0.00585	-0.00311	-2.53E^{-6}	0.99	32.4	0.015	96

Table S2. Summary of the morphological and aerodynamic properties of the natural and artificial seeds integrated with the fluorescent sensors.

	Natural seed	**Artificial seed (2X) with fluorescent sensors**
Sample	10	4-10
Mass, mg	56 ± 11	697 ± 3 (PHA seed) 6.4 ± 0.6 mg (sensors)
Wing surface, (S, mm^2)	173 ± 21	709 ± 30
Wing loading (W, N/mm^2)	3.17 ± 1.01	9.72 ± 0.55
Descent speed (v_d, m/s)	1.04 ± 0.11	1.80 ± 0.23
Rotational velocity (Ω,rad/s)	160.5 ± 23.3	144.1 ± 15.3
Wing tip speed (v_t, m/s)	3.94 ± 0.57	7.00 ± 0.79
C_D	4.87 ± 2.58	4.99 ± 1.53

References

S1. A. Nexha, J. J. Carvajal, M. C. Pujol, F. Díaz and M. Aguiló, *Nanoscale*, 2021, **13**, 7913-7987.
S2. A. Nexha, M. C. Pujol Baiges and J. J. Carvajal Martí, in *Luminescent Thermometry: Applications and Uses*, eds. J. J. Carvajal Martí and M. C. Pujol Baiges, Springer International Publishing, Cham, 2023, DOI: 10.1007/978-3-031-28516-5_6, pp. 221-268.